

OPEN

Structural design of microbicidal cationic oligomers and their synergistic interaction with azoles against *Candida albicans*

Yuan Yuan¹, Feng Zhou², Haibin Su³  & Yugen Zhang¹

Membrane-disrupting synthetic antimicrobial polymers have been well developed as antimicrobial peptide (AMP) mimics to mitigate antimicrobial resistance (AMR). However, synthetic polymers possess inherent drawbacks, being a mixture of different chain lengths, which restricts their clinical applications. In fact, synthetic oligomers with defined chain length and molecular structure could be better representatives of AMPs. Herein, a series of novel imidazolium-ammonium oligomers developed in this work exhibit excellent broad spectrum antimicrobial activity, specifically the salient structure dependent high efficiency against *C. albicans*. Moreover, synergistic effect emerged when the combined azoles and synthetic oligomers were applied against *C. albicans*. The detail structural coupling between azoles and oligomers was scrutinized through molecular dynamics simulations to unravel the interaction details with the atomistic resolution. The labile interaction between oligomer and azoles facilitated the transfer of drug into fungal cells, which can be a synergistic solution to prevent the development of resistance on *C. albicans*.

Antimicrobial resistance (AMR) is one of the major global healthcare threats^{1,2}. Its development is closely related to the overuse of antibiotics, including clinical and non-therapeutic applications³. The emergence of resistance against antibiotics is hardly surprising as antibiotics generally inhibit specific intracellular processes and resistance can be acquired by mutations in targets or related processes⁴. Antimicrobial peptides (AMPs) kill microbe via electrostatic and hydrophobic interactions which disrupt the lipid domains of cytoplasmic membrane⁵. This membrane-disrupting mechanism could prevent the development of resistance⁶. However, the high cost of manufacture, proteolytic degradation and *in vivo* toxicity limit the clinical application of AMPs. To overcome these problems, synthetic antimicrobial polymers have been well studied as AMP mimics^{7–10}. Synthetic polymers were designed to have similar amphiphilic structures non-specific membrane-targeting activity to AMPs^{11–16}. And a few AMP mimics displayed potent antifungal activity^{17–21}. Despite the excellent *in vitro* and *in vivo* antimicrobial activities, there is concern for the clinical application of synthetic polymers about the heterogeneity (a mixture of polymers with different chain lengths) and toxicity related to high molecular weight component. Instead, synthetic oligomers with defined chain length and molecular structure could be a better representation of AMPs^{22–27}. The structure parameters of oligomers, such as balanced amphiphilicity, charge density and structural flexibility, could be tailored to achieve optimum antimicrobial functionality and biocompatibility. Herein, a series of novel imidazolium-ammonium oligomers was developed. These oligomers exhibited excellent broad spectrum antimicrobial activities, including a structure dependent high activity against *C. albicans*.

Candidiasis is one of the most prevalent human opportunistic fungal infections among immunocompromised or debilitated patients^{28,29}. The largest family of antifungal drugs are azoles. Azoles are only fungi-static and their efficacy relies on the presence of cellular host defenses³⁰. Moreover, with the prolonged and extensive clinical use of azoles, drug-resistance emerged rapidly^{31,32}. These problems underlie the need for novel antifungal agents or improved therapeutic strategies. Considering that the development of new antifungal drugs is relatively slow,

¹Institute of Bioengineering and Nanotechnology, 31 Biopolis Way, The Nanos, Singapore, 138669, Singapore.

²School of Materials Science and Engineering, Nanyang Technological University, 50 Nanyang Avenue, Singapore, 639798, Singapore. ³Department of Chemistry, The Hong Kong University of Science and Technology, Hong Kong, China. Correspondence and requests for materials should be addressed to H.S. (email: haibinsu@ust.hk) or Y.Z. (email: ygzhang@ibn.a-star.edu.sg)

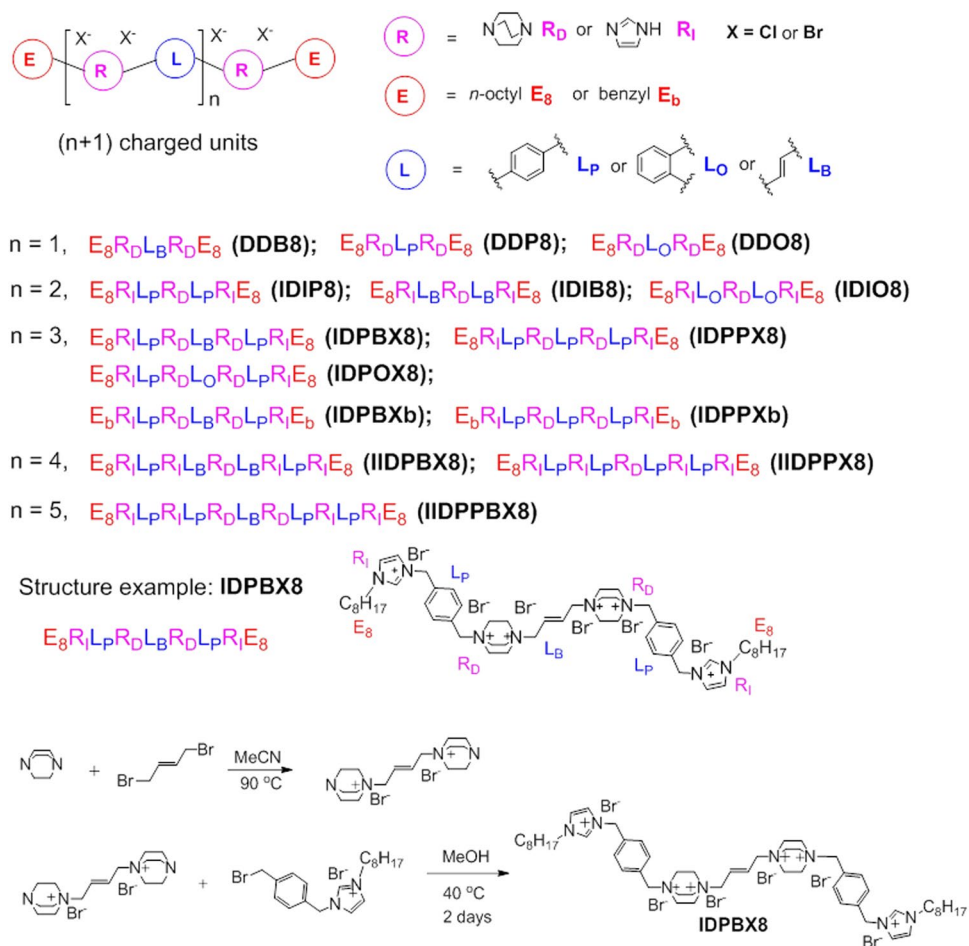


Figure 1. General formula, charge units, structure codes and structures of ammonium-imidazolium oligomers. Structure and synthesis scheme of IDPBX8.

more attentions have been paid to combination therapy³³. The antifungal combinations could enhance the rate and extent of killing, and widen the spectrum and potency of drug activity, achieving a more rapid antifungal effect and also reducing the dosage of individual drugs. In some cases, they could also minimize the development of antifungal resistance or reduce toxicity. Currently, fluconazole, the most widely used azole drug, has been studied in combination with antibiotics^{34–42} and a few non-antifungal compounds^{43–45} against *C. albicans*. In this study, combinations of azoles and synthetic oligomers were tested on *C. albicans* and the structure dependent synergistic effects were established and further investigated with molecular dynamics simulations.

Results and Discussion

Structural design of cationic oligomers. Both imidazole^{46–49} and 1,4-diazabicyclo-[2.2.2]-octane (DABCO)^{50–53} have been used as basic units to synthesize antimicrobial materials. Imidazole is a planar aromatic molecule. When both of the nitrogen atoms are substituted, the resulting imidazolium will bear a single positive charge. DABCO is a steric flexible molecule which will bear two positive charges when the two nitrogen atoms are both substituted. Herein, imidazole and DABCO are selected as synthons to construct oligomers with suitable linkers and ending groups to achieve optimum antimicrobial property by tuning their charge density, hydrophobicity and structure flexibility (Fig. 1).

Structure-activity relationship. The antimicrobial activities of oligomers were evaluated against four different clinically relevant microbes: *S. aureus*, *E. coli*, *P. aeruginosa*, and *C. albicans*, as presented in Table 1. In general, the properties of these ammonium-imidazolium oligomers are correlated to their structural components, such as linkers, ending groups, and the chain length/the number of charged units. The structure of the ending group is crucial for the antimicrobial activity. All the oligomers except **IDPPXb** exhibited strong antibacterial activity against *S. aureus* and *E. coli*. **IDPPXb**, which possesses benzyl as the ending group, showed very weak activity against the four microbes. The result was in accordance with literature that the long aliphatic ending group can enhance antimicrobial activity by facilitating the interaction between the antimicrobial compound and the cell membrane²⁶.

Besides the ending group, the central linker is also very important for their performance. When the number of charged units is 4, **IDPOX8** which has *o*-xylenyl linker in the center exhibited the greatest antibacterial activity

Sample name	MIC ($\mu\text{g mL}^{-1}$) ^a				HC ₁₀ ^b ($\mu\text{g mL}^{-1}$)	FIC ^c	CMC ($\mu\text{g mL}^{-1}$)
	S.A.	E.C.	P.A.	C.A.			
DDB8	4	4	125	125 (16)	>2000	0.25	1552
DDP8	8	4	2000	500 (31)	>2000	0.19	1896
DDO8	4	2	31	125 (16)	>2000	0.38	3038
IDIP8	2	4	500	125 (8)	>2000	0.25	985
IDIB8	8	16	500	>500 (31)	>2000	0.25	1829
IDIO8	4	4	500	62 (31)	>2000	0.25	1667
IDPBX8	2	2	62	8–31 (2–8)	>2000	0.38	1456
IDPPX8	4	8	125	62 (8–31)	>2000	0.25	1552
IDPOX8	4	8	62	125 (16)	>2000	0.25	1367
IDPBXb	31	16	500	>1000 (1000)	>2000	na	1732
IDPPXb	62	62	1000	2000 (500)	na	0.5	1860
ITPPX8	4	4	500	125 (16)	>2000	0.25	1342
IIDPBX8	4	62	250	62 (8)	>2000	0.31	291
IIDPPX8	1	2	62	125 (16)	>2000	0.38	451
IIDPPBX8	2	4	62	31 (2–8)	>2000	1.00	727
IBN-C8 ¹⁷	4	8	16	16 (2–4)	>2000	2.00	226
Fluconazole	—	—	—	>125 (2–4)	—	—	—
Itraconazole	—	—	—	>2 (0.016–0.032)	—	—	—
Voriconazole	—	—	—	>2 (0.025–0.10)	—	—	—

Table 1. Antimicrobial activity (MIC, $\mu\text{g mL}^{-1}$), the fractional inhibitory concentration index (FIC) with Fluconazole, haemolytic property (HC₁₀, $\mu\text{g mL}^{-1}$), and critical micelle concentration (CMC, $\mu\text{g mL}^{-1}$) of the ammonium-imidazolium oligomers. EC (*E. coli*), SA (*S. aureus*), PA (*P. aeruginosa*), CA (*C. albicans*), Flu (fluconazole), Itra (itraconazole), Vori (voriconazole). ^aMIC tested against $\sim 10^6$ CFU mL⁻¹ of microbes (MIC tested at $\sim 10^8$ CFU mL⁻¹ of microbes was included in SI, Table S1). The MIC was taken as the lowest concentration of the antimicrobial oligomer that no visible growth was observed by unaided eyes. For MIC tested against *C. albicans*, the lowest concentration that inhibited at least 50% fungal growth was listed in brackets. ^bHC₁₀ was taken as oligomer concentration at which the oligomer causes 10% hemolysis. ^cThe FIC of a compound with fluconazole was calculated using the lowest concentration of a compound that inhibited at least 50% fungal growth since fluconazole is fungi-static.

compared to those with *p*-xylenyl linker or *trans*-butene linker. However, **IDPBX8**, with a more flexible butene linker, was the most effective antifungal compound with MIC of 8–31 $\mu\text{g mL}^{-1}$ against *C. albicans*. A similar trend was observed when the number of charged units is 2. **DDO8** with *o*-xylenyl linker displayed lowest MIC against the three bacteria.

In addition, the length of the main-chain oligomers or the number of charged units also affects their antimicrobial property. The chain lengths of **DDB8**, **IDPBX8** and **IIDPPBX8** are different although they have similar structure components. The shortest **DDB8**, with the highest charge density, showed greatest antimicrobial activity against *S. aureus* and *E. coli*, while the long chain molecules with flexible butene linker, **IDPBX8** and **IIDPPBX8**, were more active toward *C. albicans*.

The oligomers could easily form cationic micelles in water (see Table 1). Considering that their critical micelle concentrations (CMCs) are in the range of 291 to 3038 $\mu\text{g mL}^{-1}$ which is much higher than their effective antimicrobial concentrations, the micelle formation may not have significant influence on their microbicide property. In addition, the haemolytic behaviour of the oligomers was tested over a range of concentrations (Table 1). All the oligomers did not induce noticeable haemolysis even at the highest concentration 2000 $\mu\text{g mL}^{-1}$. Considered alongside their high antimicrobial activity, these oligomers are primarily qualified as active and non-toxic compounds which display high selectivity for a wide range of pathogenic microbes over mammalian cells.

The killing efficacy of selected oligomers was evaluated against *C. albicans* at 62 $\mu\text{g mL}^{-1}$ with fluconazole as positive control (Fig. 2). After 24 h treatment with fluconazole, the growth of *C. albicans* was suppressed, indicating the fungi-static nature of fluconazole. All of the synthetic oligomers also exhibited antifungal activity. Specifically, **IDPPX8** and **DDB8** were found to be fungi-static while the other oligomers were fungicidal. **IDPBX8** killed *C. albicans* faster than others. 99% killing was observed after 24 h treatment and it increased to 99.99% after 48 h.

Synergistic effect with azoles against *C. albicans*. Azoles, more specifically triazoles, are currently the most widely used and studied class of antifungal agents. To achieve enhanced efficacy, the interaction of our synthetic oligomers with norfloxacin (an antibiotic drug for bacterial infection) and three triazoles, including fluconazole, itraconazole and voriconazole (Fig. 3) were investigated.

Firstly, the interactions of **IDPBX8** with norfloxacin or fluconazole were studied. The growth of microbes was monitored by measuring turbidity and quantified with colony counting method. From Fig. 4a,b, the combination of **IDPBX8** and norfloxacin (1:1 wt ratio) did not show improved efficacy against *S. aureus* while **IDPBX8** combined with fluconazole showed higher activity against *C. albicans* than each compound/medicine used alone. The

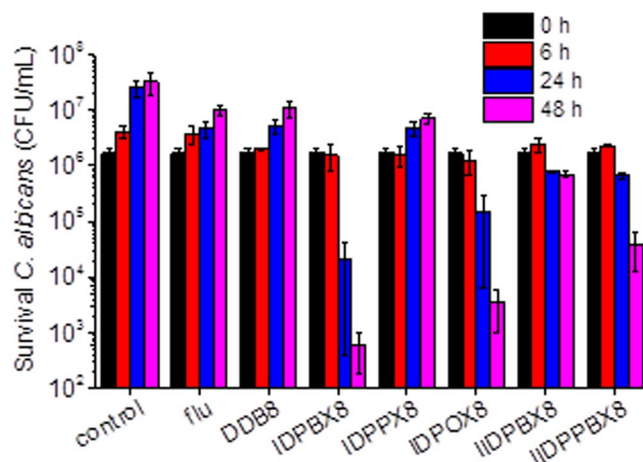


Figure 2. Antifungal activity of selected oligomers and fluconazole (flu) against *C. albicans*. Colony forming unit of *C. albicans* after treatment with oligomers at $62 \mu\text{g mL}^{-1}$ for different periods. *C. albicans* grown in Yeast Mold broth were used as control. The data are expressed as mean \pm S.D. of triplicates.

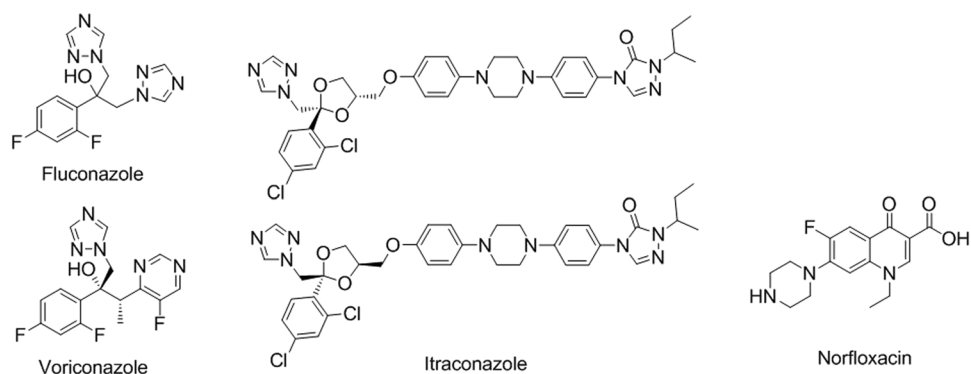


Figure 3. Structure of azoles and norfloxacin.

results of colony counting using nutrient agar plates reflected the concentration of survival *C. albicans* (Fig. 4c). Killing effect was observed when the total concentration of the combination is as low as $2 \mu\text{g mL}^{-1}$, while killing was only observed when the concentration of individual component (the oligomer used alone) reached $31 \mu\text{g mL}^{-1}$.

The interaction of the oligomers with triazoles was further studied using checkerboard dilution and time kill methods⁵⁴. The fractional inhibitory concentration (FIC) index values for the interaction of oligomers with fluconazole were reflected in Table 1. Oligomers with less than 6 charged units ($n < 5$) and *n*-octyl ending group all gave synergistic profiles when they were combined with fluconazole at sub-inhibitory concentrations. And synergistic effects were observed with at least one dose pair of combination against *C. albicans*. On the contrary, oligomers with 6 charged units ($n = 5$) and oligomers with aromatic ending groups all resulted in indifferent effects ($0.5 < \text{FIC} \leq 4$). No antagonistic effects were found in all of the combinations.

Time-kill experiments were performed with selected antifungal combinations according to the results of the checkerboard assay. Figures 4d,e illustrate the synergistic kinetics of combinations of IDPBX8 and fluconazole in the time kill assay. Combination of $1 \mu\text{g mL}^{-1}$ IDPBX8 plus $0.5 \mu\text{g mL}^{-1}$ fluconazole, and of $2 \mu\text{g mL}^{-1}$ IDPBX8 plus $0.25 \mu\text{g mL}^{-1}$ fluconazole revealed a stable and continuous inhibition of colony counts after 24 h compared to the single substance of IDPBX8 or fluconazole.

The interaction of oligomers with other triazoles, such as itraconazole and voriconazole, was also investigated using checkerboard dilution method. The FICs of different combinations against *C. albicans* were shown in Table 2. Synergy was also observed when IDPBX8 or IDPPX8 was applied together with voriconazole.

Three types of mechanism are frequently cited as resulting in synergy between two or more antifungal agents³³. The first mechanism results from sequential inhibition of different steps of a common biochemical pathway. The second proposed mechanism is simultaneous inhibition of cell wall and cell membrane targets in fungi. The third mechanism arises from simultaneous therapy with cell wall or cell membrane-active agents to enhance the penetration of a second antifungal agent. Herein, it was observed that synergistic effect occurred between fluconazole and short chain oligomers with charge units less than 6. When the charge unit of oligomer chain is 6 or more, synergy was not observed although individual components had antifungal property. These results cannot

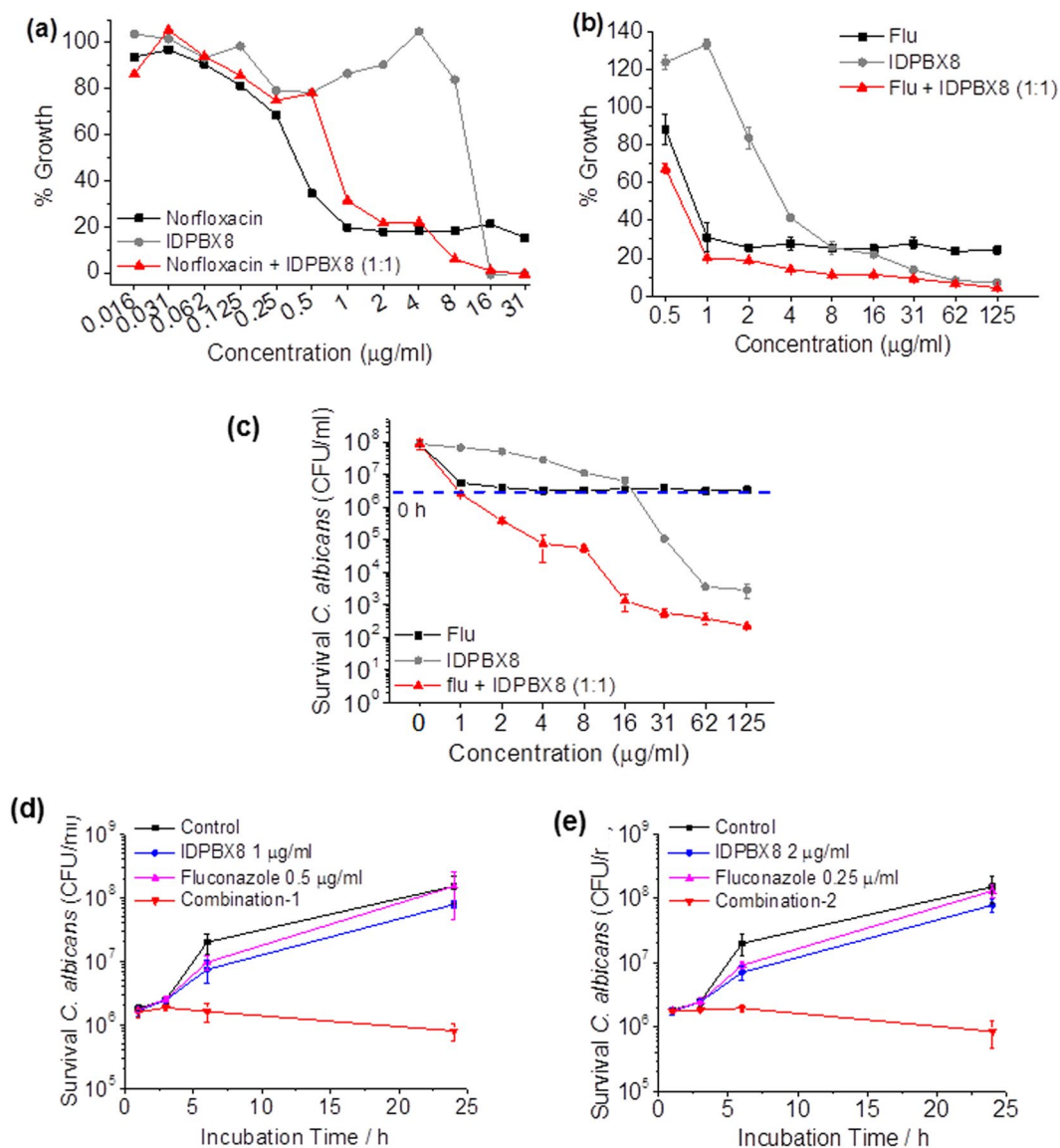


Figure 4. Synergistic effect was observed between **IDPBX8** and fluconazole, but not norfloxacin. **(a)** Growth of *S. aureus* after 24 h incubation with varied concentration of norfloxacin, **IDPBX8** and their mixture. **(b)** Growth of *C. albicans* after 24 h incubation with varied concentration of fluconazole, **IDPBX8** and their mixture. The % growth was calculated based on the absorbance at 600 nm measured by a plate reader. **(c)** Colony forming units (CFU) of *C. albicans* after 24 h incubation with varied concentration of fluconazole, **IDPBX8** and their mixture. The concentration of *C. albicans* at 0 h is 3.8×10^6 CFU mL⁻¹ as indicated in the figure as blue dash line. **(d,e)** Time-kill curve of **IDPBX8**, fluconazole alone and in combination against *C. albicans*, colony forming units (CFU) of *C. albicans* at different time after incubation with **IDPBX8** or fluconazole alone, or combinations. **(d)** Combination-1: **IDPBX8** (1 µg mL⁻¹) and fluconazole (0.5 µg mL⁻¹); **(e)** Combination-2: **IDPBX8** (2 µg mL⁻¹) and fluconazole (0.25 µg mL⁻¹). The data are expressed as mean ± S.D. of triplicates.

be simply explained by the three reported mechanisms. It is plausible that the interactions between azoles and oligomers are essential to their synergistic interaction.

To further understand the mechanism of these synergistic effects, interactions between oligomers and drug molecules were studied by molecular dynamics simulations^{55,56}. Oligomers, **DDP8** (n = 1), **IDIP8** (n = 2), **IDPBX8**, **IDPPX8**, **IIDPBX8** (n = 4), **IIDPPX8** and **IBN-C8** (n = 5) were selected for the molecular dynamics study.

The interactions between oligomers with charge units less than 6 (n < 5) and the fluconazole molecules are very labile. Figures 5 and S1–2 illustrates the equilibrium between contacted oligomer-fluconazole and separated dual. Oligomers with 6 charge units (n = 5) have much stronger interaction with fluconazole molecules. They are mostly tightly coupled in the course of simulation of 20 ns long (Table 3). The labile interaction between oligomer and drug molecule promotes synergistic effect between them. These interactions are anticipated to allow oligomers to attack cell membrane, and subsequently, facilitate the fluconazole molecules to pass through the cell

Components		MIC ^b (μg mL ⁻¹)		Combined MIC (μg mL ⁻¹)		FIC
A	B ^a	A	B	A	B	
IDPBX8	Flu	8	2	1	0.5	0.38
IDPBX8	Itra	8	0.03	1	0.015	0.62
IDPBX8	Vori	8	0.1	2	0.006	0.31
IDPPX8	Flu	16	4	2	0.25	0.19
IDPPX8	Itra	16	0.016	4	0.004	0.50
IDPPX8	Vori	16	0.025	4	0.003	0.30
IIDPPBX8	Flu	2	4	1	2	1.0

Table 2. Effect of treatments with combinations of selected oligomers and triazoles on the growth of *C. albicans* according to the FIC. ^aFlu (fluconazole), Itra (itraconazole), Vori (voriconazole). ^bMICs were the lowest concentration that inhibited at least 50% fungal growth.

Sample name	Charge units	Azoles	Interaction Index ^a	FIC
DDP8	2	Fluconazole	0.85	0.19
IDIP8	3	Fluconazole	0.09	0.25
IDPBX8	4	Fluconazole	0.44	0.38
IDPPX8	4	Fluconazole	0.61	0.25
IIDPBX8	5	Fluconazole	0.27	0.31
IIDPPBX8	6	Fluconazole	0.005	1.00
IBN-C8	6	Fluconazole	0	2.00
IDPBX8	4	Voriconazole	0.65	0.31
IDPBX8	4	Itraconazole	0	0.62

Table 3. The fractional inhibitory concentration index (FIC) and computational interactions between oligomers and azoles. ^aContact points during 20 ns trajectory between oligomers and azole molecules were counted in molecular dynamics simulations. Interaction index: counts less than 20 contacts/total counts. Interaction index less than 0.01 means very strong interactions between oligomers and azole molecules.

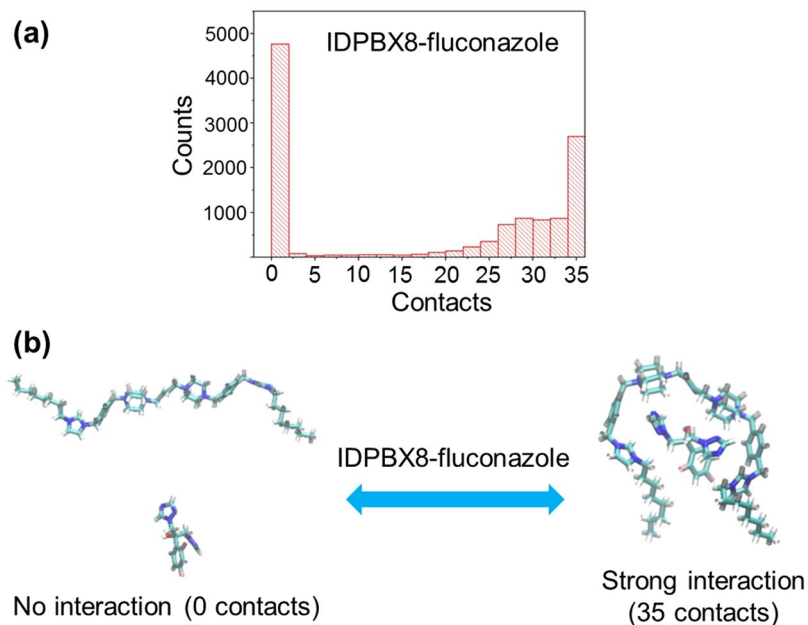


Figure 5. Interactions between IDPBX8 (A) and fluconazole (B) calculated by molecular dynamics modeling. (a) Contacts is the number of atom-atom contact within 0.6 nm between A and B. Contacts at 0 means A and B has no atom-atom contacts within 0.6 nm, in other words, A and B are separated. Counts at 35 means A and B has 35 atom-atom contacts within 0.6 nm, implying A and B are attached. (b) The figure shows molecular structures of “separated” and “attached” status and their dynamic equilibrium.

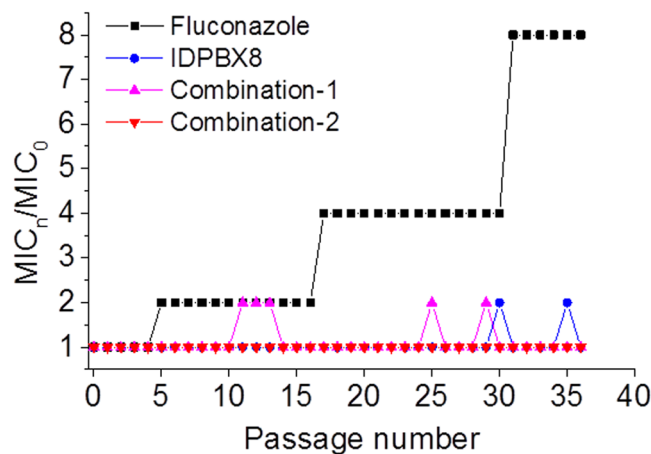


Figure 6. Resistance acquisition in the presence of $\frac{1}{4}$ MIC levels of IDPBX8, fluconazole or fluconazole-IDPBX8 combinations against *C. albicans*. Combination-1: IDPBX8 ($1 \mu\text{g mL}^{-1}$) and fluconazole ($0.5 \mu\text{g mL}^{-1}$); Combination-2: IDPBX8 ($2 \mu\text{g mL}^{-1}$) and fluconazole ($0.25 \mu\text{g mL}^{-1}$).

membrane. In contrast, the synergistic effect disappeared for those oligomer/fluconazole combinations with very strong interactions. Interestingly, antagonistic effect was also absent for these strong interactive combinations. The strong interaction between oligomer and drug molecule may hinder the release of the drug into the inner cell through translocation across the cell membrane. Similar phenomena were also observed for oligomers with other drug molecules. IDPBX8 had labile interactions with voriconazole, but strong interactions with itraconazole. Experimentally, synergistic effect was observed for IDPBX8 and voriconazole combination, while no synergy was observed for IDPBX8 and itraconazole.

Drug resistance study. Resistance to antifungal agents has been much less studied compared to antibacterial resistance⁵⁷. However, the current increase in fungal infections has intensified the exploration of innovative, safer and more efficient agents to combat fungal infections. The potential for *C. albicans* to develop resistance following repeated exposures to IDPBX8 or fluconazole-IDPBX8 combinations was investigated by serial passage of *C. albicans* treated under $\frac{1}{4}$ MIC levels for oligomer or combinations. MIC values were measured after each passage. For comparison, fluconazole was also tested. As shown in Fig. 6, the MIC of fluconazole against *C. albicans* increases at the 5th passage. By the 31th passage the MIC of fluconazole increases to 8 times of the original MIC. In contrast, the MICs of IDPBX8 and fluconazole-IDPBX8 combinations are relatively stable over the entire 36 passages, indicating that no significant resistance was developed by *C. albicans* during the 36 consecutive days of treatment with IDPBX8 or fluconazole-IDPBX8 combinations.

As we observed in Fig. 4, repeated use of oligomers alone would not induce resistance as their working mechanism involves directly destroying cell wall/membrane. Similarly, the combinations of oligomer and fluconazole could also prevent the development of resistance as the main target of their synergistic therapy is the cell membrane too. In other words, the synergistic combination therapy accelerates the delivery of fluconazole into the cell without changing its action targets.

In summary, a series of imidazolium-ammonium oligomers were synthesized and their antimicrobial activities were evaluated against bacteria and fungus. These oligomers generally have broad spectrum antimicrobial property. Among them, oligomers with more flexible linkers demonstrated higher efficiency against *C. albicans*. Structure-dependent synergistic interaction of oligomers with azoles was also established. The labile interaction between oligomer and azoles is desirable in the transfer of drug into fungal cells, thus promoting the synergistic effect. The membrane-disruption mechanism ensures oligomers and oligomers/azoles combinations to be protected from resistance development. The results reported here demonstrate a new series of promising imidazolium-ammonium oligomers which can be applied in combination with fluconazole for the treatment of fungal infections in a safer and more effective way. Our study also provides new insight into the mechanism of drug synergy interaction.

Methods

Minimum inhibitory concentration. *Staphylococcus aureus* (ATCC 6538, Gram-positive), *Escherichia coli* (ATCC 8739, Gram-negative), *Pseudomonas aeruginosa* (ATCC 9027, Gram-negative), and *Candida albicans* (ATCC 10231, fungus) were used as representative microorganisms to challenge the antimicrobial functions of the oligomers. All bacteria and fungus were frozen at -80°C , and were grown overnight at 37°C in Mueller Hinton Broth (MHB, BD Singapore) prior to experiments. Fungus was grown overnight at 22°C in Yeast Mold Broth (YMB, BD Singapore)^{27,58}. Subsamples of these cultures were grown for a further 3 h and diluted to give an optical density (O.D.) value of 0.07 at 600 nm ($\text{OD}_{600} = 0.07$), corresponding to 3×10^8 CFU mL^{-1} for bacteria and 10^6 CFU mL^{-1} for fungus (McFarland's Standard 1; confirmed by plate counts).

The oligomers were dissolved in MHB at a concentration of 4 mg mL^{-1} and the minimal inhibitory concentrations (MICs) were determined by microdilution assay. Bacterial solutions ($100 \mu\text{L}$, 10^6 CFU mL^{-1}) were mixed with $100 \mu\text{L}$ of oligomer solutions (normally ranging from 4 mg mL^{-1} to $2 \mu\text{g mL}^{-1}$ in serial two-fold dilutions) in

each well of the 96-well plate. The plates were incubated at 37 °C for 24 h with constant shaking speed at 300 rpm. The MIC measurement against *Candida albicans* was similar to bacteria except that the fungus solution was in YMB and the plates were incubated at room temperature.

The MIC was taken as the lowest concentration of the antimicrobial oligomer that no visible growth was observed by unaided eyes. For MIC test against *C. albicans*, the lowest concentration that causes at least 50% inhibition in cell growth comparing to untreated control (prominent decrease in turbidity, or score of 2, according to CLSI guidelines⁵⁹) was also recorded for further synergy study. Cell growth (i.e., the OD₆₀₀) was monitored with a microplate reader (TECAN Spark[®] 10 M, Austria). Medium solution containing microbial cells alone was used as a control (100% microbial growth). The assay was performed in four replicates and the experiments were repeated at least two times.

Monitoring the growth of *C. albicans*. The growth of *C. albicans* in the presence of IDPBX8 and fluconazole alone or their combination was monitored by measuring the absorbance at 600 nm with a microplate reader and quantified using colony counting method. Briefly, material was dissolved in YMB (2 µg mL⁻¹ to 62 µg mL⁻¹ in serial two-fold dilution). A hundred microliters of each solution were placed into a 96-well plate. Then 100 µL of *C. albicans* suspension (7.6 × 10⁶ CFU mL⁻¹) was added into each well. So the final concentration of *C. albicans* was 3.8 × 10⁶ CFU mL⁻¹. Fungus growing in pure YMB was used as control. The 96-well plate was kept on a shaker at room temperature under constant shaking. After incubation for 24 h, the absorbance of the solutions (OD₆₀₀) was measured with a plate reader and used for the calculation of the % growth using the absorbance of control solution as 100% growth. To quantify the number of viable fungi, after 24 h incubation, aliquots (100 µg mL⁻¹) were withdrawn and serially diluted with DPBS buffer (1:10). 100 µL of each dilution were spread onto nutrient agar plate (Luria-Bertani broth with 1.5% agar) and the colony forming units (CFU) were counted after incubation at room temperature for 2 days.

Checkerboard assay. In order to evaluate whether individual oligomer compounds exhibit synergy or indifference in combination with fluconazole against *C. albicans*, checkerboard assays were performed as described previously with slight modification⁶⁰. Two-fold serial dilution of oligomers and fluconazole was prepared in YMB at 4 times the strength of the final concentration ranging from 1/16 to two times of the MIC. Aliquots of 50 µL of each component at a concentration of 4 times the targeted final concentration were mixed in a 96-well plate. A row and a column in which a serial dilution of each agent was present alone were also prepared for MIC test. Then each solution in the well plate was inoculated with 100 µL of logarithmically grown 10⁶ cells mL⁻¹ *C. albicans* cells in the 96-well plate. The plate also contained a column with *C. albicans* only as control (100% cell growth). The cells were incubated at room temperature for 24 h with constant shaking, after which cell growth (i.e., the OD₆₀₀) was monitored with a plate reader.

Synergy between fluconazole and oligomers was determined by calculating the fractional inhibitory concentration index (FIC). Since fluconazole is fungal-static, the MIC used for FIC calculation was the lowest concentration of an oligomer or fluconazole that caused at least 50% reduction of cell growth. FIC was calculated as follows: $FIC = (MIC_{\text{oligomer A in combination}}/MIC_{\text{oligomer A alone}}) + (MIC_{\text{azole B in combination}}/MIC_{\text{azole B alone}})$. FIC values of ≤0.5, >0.5 to ≤4.0 and >4.0 indicated synergy, indifference, or antagonistic interactions for different combinations.

Determination of critical micelle concentration. Pyrene solution in acetone (10 µL, 6.16 × 10⁻⁵ M) was added into glass vials, following which acetone was evaporated at room temperature⁶¹. Oligomer solution in DI water (1 mL) with various concentrations ranging from 0.01 to 1000 µg mL⁻¹ was added into the glass vials, giving a final pyrene concentration of 6.16 × 10⁻⁷ M and the solutions were kept overnight. The excitation spectra of the solutions were scanned from 300 nm to 360 nm with an emission wavelength of 395 nm. Both the excitation and emission bandwidths were set at 2.5 nm. The intensity ratios (I₃₃₇/I₃₃₄) were plotted against oligomer concentration. The CMC value was given by the intersection of the tangent to the curve at the inflection and the tangent of the points at low oligomer concentrations.

Time-kill method. Time-kill experiments were performed with selected antifungal combinations based on the results of the checkerboard assay^{47,48}. IDPBX8 and fluconazole were tested alone and in combination at sub-MIC level (below original MIC values). The mixtures were inoculated with *C. albicans* and adjusted to give a final concentration of about 10⁶ CFU mL⁻¹. After 1, 3, 6 and 24 h incubation at room temperature, the respective cell suspensions were collected (100 µL), serially diluted as 1:10, and 100 µL of each dilution was spread on Luria-Bertani agar. Colonies were counted after 48 h incubation at room temperature and the CFU mL⁻¹ was calculated accordingly.

Resistance studies. Drug resistance was induced by treating *C. albicans* repeatedly with IDPBX8, IDPBX8-fluconazole combination or fluconazole⁵⁸. Firstly, MICs of the tested compounds were determined against *C. albicans* using the broth microdilution method. Then, serial passaging was initiated by transferring microbial suspension grown at the sub-MIC of the copolymers (1/4 of MIC at that passage) for another MIC assay. After 24 h incubation, cells grown at the 1/4-MIC of the test compounds were once again transferred and assayed for MIC. The MIC was tested for 36 passages. Drug-resistant behavior was evaluated by recording the changes in the MIC normalized to that of the first passage.

Haemolysis study. Fresh mouse red blood cells (RBCs) were diluted with PBS buffer to give a RBC stock suspension (4 vol% blood cells)⁵⁸. 100 µL aliquots of RBC suspension were mixed with 100 µL oligomer solutions of various concentrations (ranging from 4 mg mL⁻¹ to 2 µg mL⁻¹ in serial two-fold dilutions in PBS). After 1 h incubation at 37 °C, the mixture was centrifuged at 2000 rpm for 5 min. Aliquots (100 µL) of the supernatant were transferred to a 96-well plate. Haemolytic activity was determined as a function of haemoglobin release by

measuring absorbance of the supernatant at 576 nm using a microplate reader. A control solution that contained only PBS was used as a reference for 0% haemolysis. Absorbance of red blood cells lysed with 0.5% Triton-X was taken as 100% haemolysis. The data were expressed as mean and S.D. of four replicates.

$$\% \text{ Haemolysis} = [\text{OD}_{576\text{nm}} (\text{polymer}) - \text{OD}_{576\text{nm}} (\text{PBS})] / [\text{OD}_{576\text{nm}} (\text{Triton-X}) - \text{OD}_{576\text{nm}} (\text{PBS})] \times 100\%$$

HC₁₀ was taken as oligomer concentration at which the oligomer causes 10% hemolysis.

Statistical analysis. Data were expressed as means \pm standard deviation of the mean (S.D. is indicated by error bars)⁵⁸. Student's *t*-test was used to determine significance among groups. A difference with *p* < 0.05 was considered statistically significant.

Computational method. All molecular dynamics simulations were performed using the GROMACS 4.5.3 suite of programs^{27,47}. The amber03 force field was used to describe the drug and oligomer molecules. Water molecules were described using the TIP5P water model. The overall temperature of 300 K was modulated with Nose-Hoover thermostat. The integration of the equations of motion was performed by using a leap frog algorithm with a time step of 1 fs. Periodic boundary conditions were implemented in all systems. A cutoff of 1 nm was implemented for the Lennard-Jones and the direct space part of the Ewald sum for Coulombic interactions. The Fourier space part of the Ewald splitting was computed by using the particle-mesh-Ewald method, with a grid length of 0.16 nm on the side and a cubic spline interpolation. Each sample was run for 20 ns. The initial coordinates of the drug and oligomer molecules were made from Gaussview and optimized by density functional theory using M06-2X functional and 6-31 g(d) basis set as built in Gaussian 09 package.

References

1. Review on Antimicrobial resistance: Tackling a crisis for the health and wealth of nations, Chaired by O'Neill, J. HM Government (2014).
2. Levy, S. B. & Marshall, B. Antibacterial resistance worldwide: causes, challenges and responses. *Nat. Med.* **10**, S122–129 (2004).
3. World Health Organization, Fact sheet, Antimicrobial resistance, <http://www.who.int/mediacentre/factsheets/fs194/en/> "reports of bacterial infections by strains resistant to all existing drugs"
4. Rice, L. B. Federal funding for the study of antimicrobial resistance in nosocomial pathogens: no ESCAPE. *J. Infect. Dis.* **197**, 1079–1081 (2008).
5. Hancock, R. E. W. & Sahl, H.-G. Antimicrobial and host-defense peptides as new anti-infective therapeutic strategies. *Nat. Biotechnol.* **24**, 1551–1557 (2006).
6. Mangoni, M. L., McDermott, A. M. & Zasloff, M. Antimicrobial peptides and wound healing: biological and therapeutic considerations. *Exp. Dermatol.* **25**, 167–173 (2006).
7. Mahlapuu, M., Håkansson, J., Ringstad, L. & Björn, C. Antimicrobial peptides: an emerging category of therapeutic agents. *Front. Cell. Infect. Microbiol.* **6**, 194–199 (2016).
8. Sgolastra, F., deRonde, B. M., Sarapas, J. M., Som, A. & Tew, G. N. Designing mimics of membrane active proteins. *Acc. Chem. Res.* **46**, 2977–2987 (2013).
9. Findlay, B. G., Zhanel, G. & Schweizer, F. Cationic Amphiphiles, A new generation of antimicrobials inspired by the natural antimicrobial peptide scaffold. *Antimicrob. Agents Chemother.* **54**, 4049–4058 (2010).
10. Konai, M. M., Bhattacharjee, B., Ghosh, S. & Haldar, J. Recent progress in polymer research to tackle infections and antimicrobial resistance. *Biomacromolecules* **19**, 1888–1917 (2018).
11. Xu, H. *et al.* Green fabrication of amphiphilic quaternized β -chitin derivatives with excellent biocompatibility and antibacterial activities for wound healing. *Adv. Mater.* **30**, 1801100 (2018).
12. Ganewatta, M. S. & Tang, C. B. Controlling macromolecular structures towards effective antimicrobial polymers. *Polymer* **63**, A1eA29 (2015).
13. Engler, A. C. *et al.* Emerging trends in macromolecular antimicrobials to fight multi-drug-resistant infections. *Nano Today* **7**, 201–222 (2012).
14. Tew, G. N. *et al.* De novo design of biomimetic antimicrobial polymers. *Proc. Natl. Acad. Sci. USA* **99**, 5110–5114 (2002).
15. Sambhy, V., Peterson, B. R. & Sen, A. Antibacterial and Hemolytic Activities of Pyridinium Polymers as a Function of the Spatial Relationship between the Positive Charge and the Pendant Alkyl Tail. *Angew. Chem.-Int. Ed.* **47**, 1250–1254 (2008).
16. Kuroda, K., Caputo, G. A. & DeGrado, W. F. The role of hydrophobicity in the antimicrobial and hemolytic activities of polymethacrylate derivatives. *Chem.-Eur. J.* **15**, 1123–1133 (2009).
17. Durnaš, B. *et al.* Candidacidal Activity of Selected Ceragenins and Human Cathelicidin LL-37 in Experimental Settings. *PLoS ONE* **11**, e0157242 (2016).
18. Sader, H. S., Fedler, K. A., Rennie, R. P., Stevens, S. & Jones, R. N. Omiganan pentahydrochloride (MBI 226), a topical 12-amino-acid cationic peptide: spectrum of antimicrobial activity and measurements of bactericidal activity. *Antimicrob. Agents Chemother.* **48**, 3112–3118 (2004).
19. Chongsiriwatana, N. P. *et al.* Short Alkylated Peptoid Mimics of Antimicrobial Lipopeptides. *Antimicrob. Agents Chemother.* **55**, 417–420 (2011).
20. Duggineni, S. *et al.* A novel dodecapeptide from a combinatorial synthetic library exhibits potent antifungal activity and synergy with standard antimycotic agents. *Int. J. Antimicrob. Agents* **29**, 73–78 (2007).
21. Menzel, L. P. *et al.* Potent *in vitro* and *in vivo* antifungal activity of a small molecule host defense peptide mimic through a membrane-active mechanism. *Sci. Rep.* **7**, 4353 (2017).
22. Liu, D. *et al.* Nontoxic membrane-active antimicrobial arylamide oligomers. *Angew. Chem. Int. Ed.* **43**, 1158–1162 (2004).
23. Porel, M., Thornlow, D. N., Phan, N. N. & Alabi, C. A. Sequence-defined bioactive macrocycles via an acid-catalysed cascade reaction. *Nat. Chem.* **8**, 590–596 (2016).
24. Zhou, Z. *et al.* Sequence and dispersity are determinants of photodynamic antibacterial activity exerted by peptidomimetic oligo(thiophene)s. *ACS Appl. Mater. Interfaces* **11**, 21896–1906 (2019).
25. Ergene, C., Yasuhara, K. & Palermo, E. F. Biomimetic antimicrobial polymers: recent advances in molecular design. *Polym. Chem.* **9**, 2407–2427 (2018).
26. Riduan, S. N. *et al.* Ultrafast killing and self-gelling antimicrobial imidazolium oligomers. *Small* **12**, 1928–1934 (2016).
27. Yuan, Y. & Zhang, Y. Synthesis of imidazolium oligomers with planar and stereo cores and their antimicrobial applications. *ChemMedChem* **12**, 835–840 (2017).
28. Pfaller, M. A. & Diekema, D. J. Epidemiology of invasive candidiasis: a persistent public health problem. *Clin. Microbiol. Rev.* **20**, 133–163 (2007).

29. Wilson, L. S. *et al.* The direct cost and incidence of systemic fungal infections. *Value Health* **5**, 26–34 (2002).
30. Spampinato, C. & Leonardi, D. Candida infections, causes, targets, and resistance mechanisms: Traditional and alternative antifungal agents. *Biomed. Res. Int.* **2013**, 204237 (2013).
31. White, T. C., Holleman, S., Dy, F., Mirels, L. F. & Stevens, D. A. Resistance mechanisms in clinical isolates of *Candida albicans*. *Antimicrob. Agents Chemother.* **46**, 1704–1713 (2002).
32. Niimi, M., Firth, N. A. & Cannon, R. D. Antifungal drug resistance of oral fungi. *Odontology* **98**, 15–25 (2010).
33. Lewis, R. E. & Kontoyiannis, D. P. Rationale for combination antifungal therapy. *Pharmacotherapy* **21**, 149S–164S (2001).
34. Johnson, M. D., MacDougall, C., Ostrosky-Zeichner, L., Perfect, J. R. & Rex, J. H. Combination antifungal therapy. *Antimicrob. Agents Chemother.* **48**, 693–715 (2004).
35. Barchiesi, F., Francesco, L. F. D. & Scalise, G. *In vitro* activities of terbinafine in combination with fluconazole and itraconazole against isolates of *Candida albicans* with reduced susceptibility to azoles. *Antimicrob. Agents Chemother.* **41**, 1812–1814 (1997).
36. Ghannoum, M. & Elewski, B. Successful treatment of fluconazole resistant oropharyngeal candidiasis by a combination of fluconazole and terbinafine. *Clin. Diagn. Lab Immunol.* **6**, 921–923 (1999).
37. Perea, S., Gonzalez, G., Fothergill, A. W., Sutton, D. A. & Rinaldi, M. G. *In vitro* activities of terbinafine in combination with fluconazole, itraconazole, voriconazole, and posaconazole against clinical isolates of *Candida glabrata* with decreased susceptibility to azoles. *J. Clin. Microbiol.* **40**, 1831–1833 (2002).
38. Scheid, L. A., Mario, D. A. N., Kubiça, T. F., Santurio, J. M. & Alves, S. H. *In vitro* activities of antifungal agents alone and in combination against fluconazole susceptible and resistant strains of *Candida dubliniensis*. *Braz. J. Infect. Dis.* **16**, 78–81 (2012).
39. Johnson, M. D. & Perfect, J. R. Use of antifungal combination therapy: Agents, order, and timing. *Curr. Fungal Infect. Rep.* **4**, 87–95 (2010).
40. Marchetti, O. *et al.* Fluconazole plus cyclosporine: A fungicidal combination effective against experimental endocarditis due to *Candida albicans*. *Antimicrob. Agents Chemother.* **44**, 2932–2938 (2000).
41. Shrestha, S. K., Fosso, M. Y. & Garneau-Tsodikova, S. A combination approach to treating fungal infections. *Scientific Reports* **5**, 17070 (2015).
42. Li, D.-D. *et al.* Fluconazole assists berberine to kill fluconazole-resistant *Candida albicans*. *Antimicrob. Agents and Chemother.* **57**, 6016–6027 (2013).
43. Liu, S. *et al.* Synergistic effect of fluconazole and Calcium channel blockers against resistant *Candida albicans*. *PLoS ONE* **11**, e0150859 (2016).
44. Li, X. *et al.* Potential targets for antifungal drug discovery based on growth and virulence in *Candida albicans*. *Antimicrob. Agents and Chemother.* **59**, 5885–5891 (2015).
45. Reis de Sá, L. F. *et al.* Synthetic organotellurium compounds sensitize drug-resistant *Candida albicans* clinical isolates to fluconazole. *Antimicrob. Agents Chemother.* **61**, e01231–16 (2017).
46. Riduan, S. N. & Zhang, Y. Imidazolium salts and their polymeric materials for biological applications. *Chem. Soc. Rev.* **42**, 9055–9070 (2013).
47. Liu, L., Wu, H., Riduan, S. N., Ying, J. Y. & Zhang, Y. Short imidazolium chains effectively clear fungal biofilm in keratitis treatment. *Biomaterials* **34**, 1018–1023 (2013).
48. Liu, L. *et al.* Main-chain imidazolium oligomer material as a selective biomimetic antimicrobial agent. *Biomaterials* **33**, 8625–8631 (2012).
49. Sharma, A., Wilson, G. R. & Dubey, A. Antibacterial activity of vinyl imidazole(VI) functionalized silica polymer nanocomposites (SBA/VI) against Gram negative and Gram positive bacteria. *New J. Chem.* **40**, 764–769 (2016).
50. Herman, J. L. *et al.* Synthesis, antifungal activity, and biocompatibility of novel 1,4-diazabicyclo[2.2.2]octane (DABCO) compounds and DABCO-containing denture base resins. *Antimicrob. Agents Chemother.* **61**, e02575–16 (2017).
51. Pappas, H. C. *et al.* Antifungal properties of cationic phenylene ethynyls and their impact on β -glucan exposure. *Antimicrob. Agents Chemother.* **60**, 4519–4529 (2016).
52. Dizman, B., Elasmri, M. O. & Mathias, L. J. Synthesis and antimicrobial activities of new water-soluble bis-quaternary ammonium methacrylate polymers. *J. Appl. Polym. Sci.* **94**, 635–642 (2004).
53. Mayr, J., Bachl, J., Schlossmann, J. & Díaz, D. D. Antimicrobial and hemolytic studies of a series of polycations bearing quaternary ammonium moieties: Structural and topological effects. *Int. J. Mol. Sci.* **18**, 303 (2017).
54. Singh, P. K., Tack, B. F., Mccray, P. B. Jr. & Welsh, M. J. Synergistic and additive killing by antimicrobial factors found in human airway surface liquid. *Am. J. Physiol. Lung Cell Mol. Physiol.* **279**, L799–L805 (2000).
55. Van der Spoel, D. *et al.* GROMACS: fast, flexible, and free. *J. Computational Chem.* **26**, 1701–1718 (2005).
56. Duan, Y. *et al.* A point-charge force field for molecular mechanics simulations of proteins based on condensed-phase quantum mechanical calculations. *J. Computational Chem.* **24**, 1999–2012 (2003).
57. Srinivasan, A., Lopez-Ribot, J. L. & Ramasubramanian, A. K. Overcoming antifungal resistance. *Drug Discov Today Technol.* **11**, 65–71 (2014).
58. Yuan, Y. *et al.* pH-Degradable imidazolium oligomers as antimicrobial materials with tuneable loss of activity. *Biomater. Sci.* **7**, 2317–2325 (2019).
59. Clinical and Laboratory Standards Institute. Reference method for broth dilution antifungal susceptibility testing of yeasts; approved standard-third edition; CLSI document M27-A3. Clinical and Laboratory Standards Institute, Wayne, PA, USA 2008.
60. Attia, A. B. E. *et al.* The effect of kinetic stability on biodistribution and anti-tumor efficacy of drug-loaded biodegradable polymeric micelles. *Biomaterials* **34**, 3132–3140 (2013).
61. Herce, H. D., Garcia, A. E. & Cardoso, M. C. Fundamental Molecular Mechanism for the Cellular Uptake of Guanidinium-Rich Molecules. *J. Am. Chem. Soc.* **136**, 17459–17467 (2014).

Acknowledgements

This work was supported by the Institute of Bioengineering and Nanotechnology, Biomedical Research Council, Agency for Science, Technology and Research. The work was also supported in part by Society of Interdisciplinary Research (SOIRÉE), HKUST Grants (IGN17SC04; R9418). We thank A*STAR Computational Resource Centre for providing the access to its high performance computing facilities.

Author Contributions

Y.Y. conceived the project, conducted experiment and wrote the manuscript, F.Z. conducted computational study, H.S. conceived the project, Y.Z. conceived the project and revised manuscript.

Additional Information

Supplementary information accompanies this paper at <https://doi.org/10.1038/s41598-019-48322-x>.

Competing Interests: The authors declare no competing interests.

Publisher's note: Springer Nature remains neutral with regard to jurisdictional claims in published maps and institutional affiliations.



Open Access This article is licensed under a Creative Commons Attribution 4.0 International License, which permits use, sharing, adaptation, distribution and reproduction in any medium or format, as long as you give appropriate credit to the original author(s) and the source, provide a link to the Creative Commons license, and indicate if changes were made. The images or other third party material in this article are included in the article's Creative Commons license, unless indicated otherwise in a credit line to the material. If material is not included in the article's Creative Commons license and your intended use is not permitted by statutory regulation or exceeds the permitted use, you will need to obtain permission directly from the copyright holder. To view a copy of this license, visit <http://creativecommons.org/licenses/by/4.0/>.

© The Author(s) 2019